Available online at www.sciencedirect.com
SciVerse ScienceDirect
Energy Procedia 37 (2013) 6587 – 6594
Energy Procedia

GHGT-11

Integrated geothermal-CO_2 reservoir systems: Reducing carbon intensity through sustainable energy production and secure CO_2 storage

Thomas A. Buscheck[a]*, Thomas R. Elliot[b], Michael A. Celia[b], Mingjie Chen[a], Yunwei Sun[a], Yue Hao[a], Chuanhe Lu[a], Thomas J. Wolery[a], and Roger D. Aines[a]

[a]*Lawrence Livermore National Laboratory, P.O. Box 808, L-223, Livermore CA, USA*
[b]*Department of Civil and Environmental Engineering, Princeton University, Princeton, NJ, USA*

Abstract

Large-scale geologic CO_2 storage (GCS) can be limited by overpressure, while geothermal energy production is often limited by pressure depletion. We investigate how synergistic integration of these complementary systems may enhance the viability of GCS by relieving overpressure, which reduces pore-space competition, the Area of Review, and the risks of CO_2 leakage and induced seismicity, and by producing geothermal energy and water, which can defray parasitic energy and water costs of CO_2 capture.

Selection and/or peer-review under responsibility of GHGT

Keywords: Geologic CO_2 storage; hot sedimentary aquifer; geothermal energy; pressure management; Area of Review; brine utilization

1. Introduction

Geothermal energy and geologic CO_2 storage (GCS) have the potential of significantly contributing to lowering atmospheric CO_2 emissions, which is necessary for mitigating climate change [1,2]. For large-scale CO_2 injection in saline formations, overpressure can limit the ability to store CO_2, while geothermal energy production can be limited by pressure depletion [3,4]. These two complementary systems can be integrated synergistically, with CO_2 injection providing pressure support to maintain the productivity of geothermal wells, while the net loss of brine provides pressure relief and improved injectivity for CO_2-injection wells. The loss of brine can occur as an outcome of geothermal operations [4] and/or be engineered through the consumptive beneficial use of brine for either freshwater generation or for saline cooling purposes [5,6]. Relief of overpressure can increase CO_2 storage capacity, reduce the risks of induced seismicity, as well as decrease CO_2 and brine leakage [6,7]. Depending on reservoir conditions, injected CO_2 can also be utilized as a more efficient working fluid (than brine) for geothermal heat extraction [8-10]. We examine a range of pressure-management strategies for integrating GCS with the production of geothermal energy and water in permeable saline aquifers.

* Corresponding author. Tel: +1-925-423-9390; fax: +1-925-423-0153.
E-mail address: buscheck1@llnl.gov

1876-6102
Selection and/or peer-review under responsibility of GHGT
doi:10.1016/j.egypro.2013.06.591

2. Background

For large-scale deployment of GCS in saline aquifers to be achievable, several implementation barriers must be addressed. CO_2 capture costs, sequestration safety, and public acceptance have been recognized for a number of years [1]. Receiving more recent attention are water-use demands from CO_2 capture, pore-space competition with emerging activities, such as shale-gas production, and induced seismicity [11,12]. Besides parasitic energy and water costs associated with CO_2 capture, the primary technical driver for the most challenging implementation barriers is overpressure caused by CO_2 injection.

Utilization of CO_2 to generate economic benefits is motivated by the need to defray CO_2 capture and sequestration costs. Compared to the several decades of experience with CO_2-enabled enhanced oil recovery (EOR), utilization of CO_2 in geothermal energy production has only recently been investigated [3,4,8-10]. Reservoir studies of integrated geothermal-GCS fall under two end-member approaches to CO_2 utilization. The first approach has emphasized utilization of CO_2 as an efficient working fluid because of its advantageous thermo-physical properties, namely the low viscosity and thermosyphon effect of CO_2, which reduce the parasitic power consumption of the working-fluid recirculation system [8-10]. Those studies have focused on small injector/producer well spacing in order to promote early CO_2 breakthrough and recirculation. Because the goal of the first approach is to maximize the heat-extraction benefit per ton of delivered (captured) CO_2, GCS is an ancillary, rather than a primary benefit. The second approach has emphasized utilizing CO_2 injection as a means of providing pressure support for geothermal production wells, rather than utilizing CO_2 as a working fluid [3,4]. For the second approach it is important to delay CO_2 breakthrough at the brine producers in order to maximize their useful lifetime. Hence, those studies have emphasized large injector/producer spacing. A key objective is for brine production, together with its consumptive beneficial use, to provide pressure relief for CO_2 injection, thereby increasing CO_2 storage capacity and efficiency, while reducing (1) pore-space competition with neighboring subsurface activities, (2) the Area of Review (AoR), and (3) environmental risks associated with overpressure [6,7]. A significant ancillary benefit of the second approach is that it can generate large quantities of product water (freshwater of saline cooling water) and thereby defray the parasitic water demand of CO_2 capture.

Ideal settings for GCS are deep sedimentary formations, such as sandstones, which are highly porous and permeable and laterally extensive, overlain by an impermeable laterally-extensive caprock [12]. If temperatures are high enough, such settings are also ideal for integrated geothermal-GCS. Such settings are also well suited for geothermal energy production because the caprock prevents cooler overlying water from being drawn down to the producers [3,4] and laterally extensive, highly permeable formations are conducive to high well productivity and lower hydraulic drawdown, which allows for greater spacing between producers and injectors.

3. Model description

In this study we used the NUFT code, which simulates multi-phase heat and mass flow and reactive transport in porous media [13]. A 3-D model with quarter symmetry is used to represent a 250-m-thick storage aquifer (Fig. 1), with a permeability of 10^{-13} m^2, similar to previous studies [4]. The bottom of the storage aquifer is located either 2.5 or 5.0 km below the ground surface, and is bounded by impermeable (10^{-18} m^2) (caprock and bedrock) *seal* units. The bedrock, which extends to the lower boundary 1 km below the bottom of the storage aquifer, has a no-mass-flow condition and a specific geothermal heat flux of either 75 or 100 mW/m^2. Above the storage aquifer is a sequence that includes the lower caprock (250 m thick), the middle (saline) aquifer (250 m thick), the upper caprock (250 m thick), and the upper (saline) aquifer, which extends to the ground surface (Fig. 1). Note that we did not discretely represent shallow freshwater aquifers. We also considered cases where the middle aquifer is overlain by a caprock that extends to the ground surface. Overpressure in the storage aquifer and lower caprock was found to be insensitive to whether the upper caprock is 250 m thick or extends all the way to the ground surface. A thermal conductivity of 2.0 W/m ^oC is applied throughout the model, resulting in thermal

gradients of 37.5 and 50 °C/km. The outer boundaries have a no-flow condition to represent a semi-closed reservoir with an area of 31,416 km^2. Additional model details are given elsewhere [4].

We modeled symmetrical patterns of horizontal wells, oriented orthogonal to the cross sections in Figs. 1 and 2. For all cases (Table 1), there are two horizontal CO_2 injectors at the bottom of the storage aquifer, each with a perforated length of 4 km. The total CO_2 injection rate is 480 kg/sec (15.15 million tonnes/yr) for 100 years, which is the CO_2 generated by 1.9 GWe of coal power plants. For the large well-spacing cases, CO_2 injectors are spaced 7 km from the center of injection. We also considered small well-spacing cases with CO_2 injectors spaced 2 km from the center of injection. In addition to the horizontal-well injection-only case (I-H), we considered a corresponding case (I-V) with two vertical CO_2 injectors. For the large well-spacing cases with brine production (Fig. 1b and d), four producers are spaced 2 km from the center of injection (5 km from the CO_2 injectors) at the bottom of the storage aquifer. For the small well-spacing cases, the producers are 1 km from the center of injection (1 km from the CO_2 injectors). Because fluid production is limited by the capacity of submersible pumps, we used four producers, each with a production rate of 120 kg/sec and a perforated length of 1 km. Initially, production is limited to brine; however, as CO_2 breaks through, CO_2 and brine are co-produced, with the CO_2 cut (fraction) increasing with time (Fig. 3a). Total fluid production rate (brine plus CO_2) is fixed at 120 kg/sec per well. In addition to pressure management reasons, this well pattern is motivated by the need to centralize fluid production, which minimizes the distance that hot fluids are conveyed to the geothermal plant. All produced fluid is reinjected, with produced brine injected in the brine injectors (Fig. 1b and d), and produced CO_2 returned to the CO_2 injectors. CO_2 and produced brine are injected at a fluid enthalpies corresponding to 16 °C at injection conditions, approximating average annual surface temperatures.

Table 1. Large (5-km) CO_2-injector-producer spacing cases are summarized. Small (1-km) CO_2-injector-producer spacing was also applied to B-3.

Case	Production/ injection mass ratio	Net mass injection rate (kg/sec)	Product water generation rate (acre-ft/yr)	CO_2-injector-to-brine-injector spacing	Brine injectors in overlying saline aquifer	Brine-injection-to-production mass ratio	Number of brine producers
I-V	0	480	N/A	N/A	N/A	N/A	N/A
I-H	0	480	N/A	N/A	N/A	N/A	N/A
B-1	1	480	0.0	3 km	0	1.0	0
B-2	1	480	0.0	3 km	2	1.0	0
B-3	1	480	0.0	6 km	2	1.0	0
B-4	1	316.8	4,175	3 km	2	0.66	0
3B-1	3	-9.6	12,526	3 km	4	0.66	8
3B-2	3	-9.6	12,526	3 km	4	0.66	8
4B-1	4	-172.8	16,701	3 km	4	0.66	12

Case B-1 injects all produced brine into two brine injectors at the top of the storage aquifer (Fig. 1b and d). Cases B-2, B-3, B-4, 3B-1, 3B-2, and 4B-1 also include two brine injectors at the bottom of the overlying (middle) aquifer (Fig. 2a and c), where half the produced brine is injected. For cases B-4, 3B-1, 3B-2, and 4B-1, 34 percent of the produced brine is consumed for beneficial use, such as reverse osmosis desalination or saline cooling water, and the remaining 66 percent (residual brine) injected into the storage and middle aquifers. For cases 3B-1, 3B-2, and 4B-1, a total of eight *perimeter* brine producers (each at a rate of 120 kg/sec) are added at the bottom of the middle and storage aquifers, 5 km from the brine injectors (Fig. 2b and d). The purpose of the additional brine producers is to reduce net fluid injection, which reduces overpressure in the storage aquifer and lower caprock, as well as in the far-field. For cases 3B-1, 3B-2, and 4B-1, two brine injectors are added at the bottom of the middle aquifer, above the central producers, in order to more evenly distribute brine injection. Case 3B-2 is modified from 3B-1 by injecting two-thirds (rather than half) of the residual brine into the middle aquifer and the remaining one-third into the storage aquifer. Case 4B-1 is modified from 3B-1 by adding four perimeter brine producers (each at a rate of 120 kg/sec) at the bottom of the storage aquifer (in line with the other brine producers) and by injecting 60 percent (rather than half) of the residual brine into the middle aquifer and 40 percent into the storage aquifer.

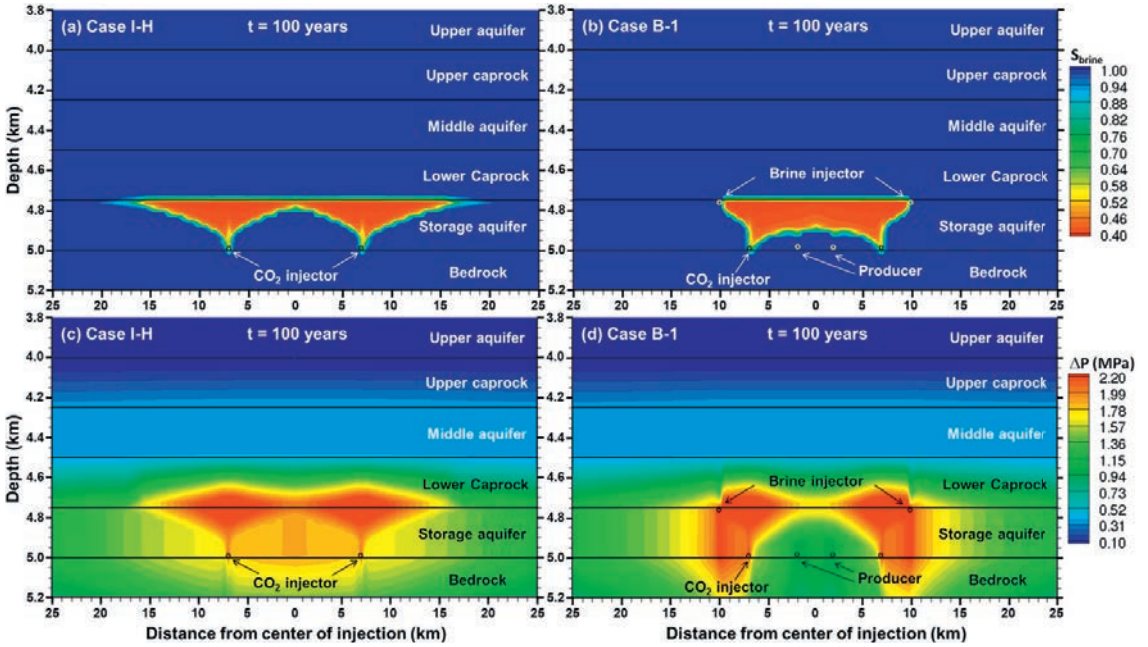

Fig.1 Brine saturation (a,b) and overpressure (c,d) for cases I-H and B-1 and a specific geothermal heat flux of 100 mw/m^2.

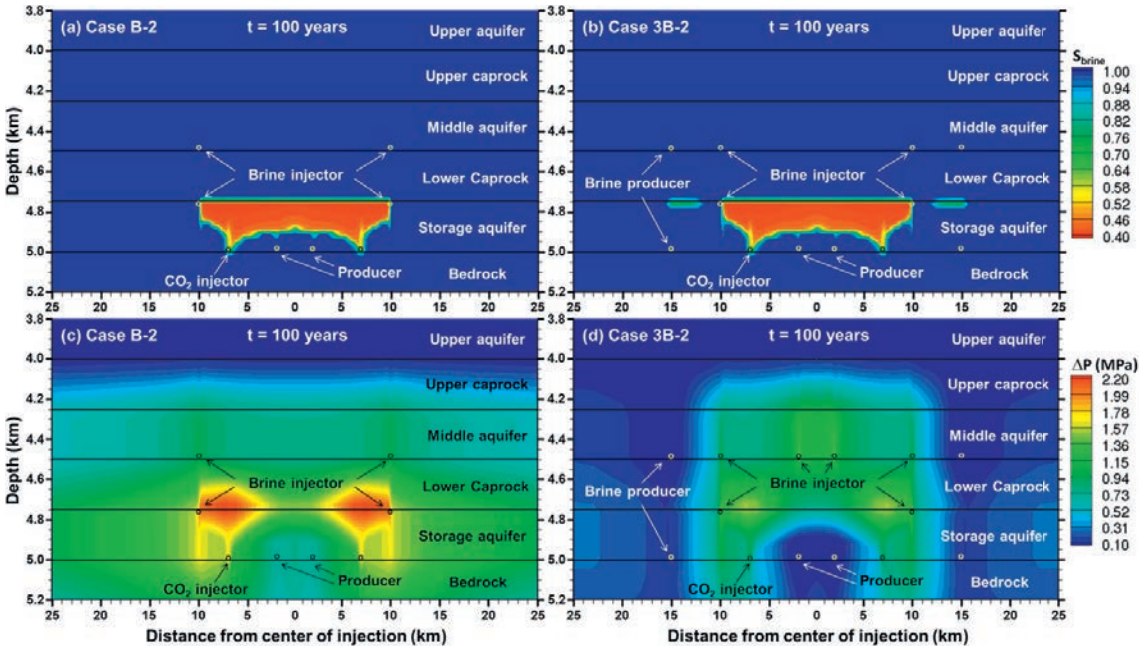

Fig. 2 Brine saturation (a,b) and overpressure (c,d) for cases B-2 and 3B-2 and a specific geothermal heat flux of 100 mw/m^2.

4. Results

Brine production and injection can achieve several useful objectives: (1) control of the CO_2 plume, (2) vertically extending and shaping the region of overpressure, which reduces the magnitude of overpressure (Fig. 4) and creates a hydraulic barrier to CO_2 leakage, (3) reducing the overpressure difference across the lower caprock (Fig. 5),

which also reduces the potential for CO_2 leakage, (4) reducing far-field overpressure (Fig. 6), and (5) producing large quantities of brine for generating water and electricity.

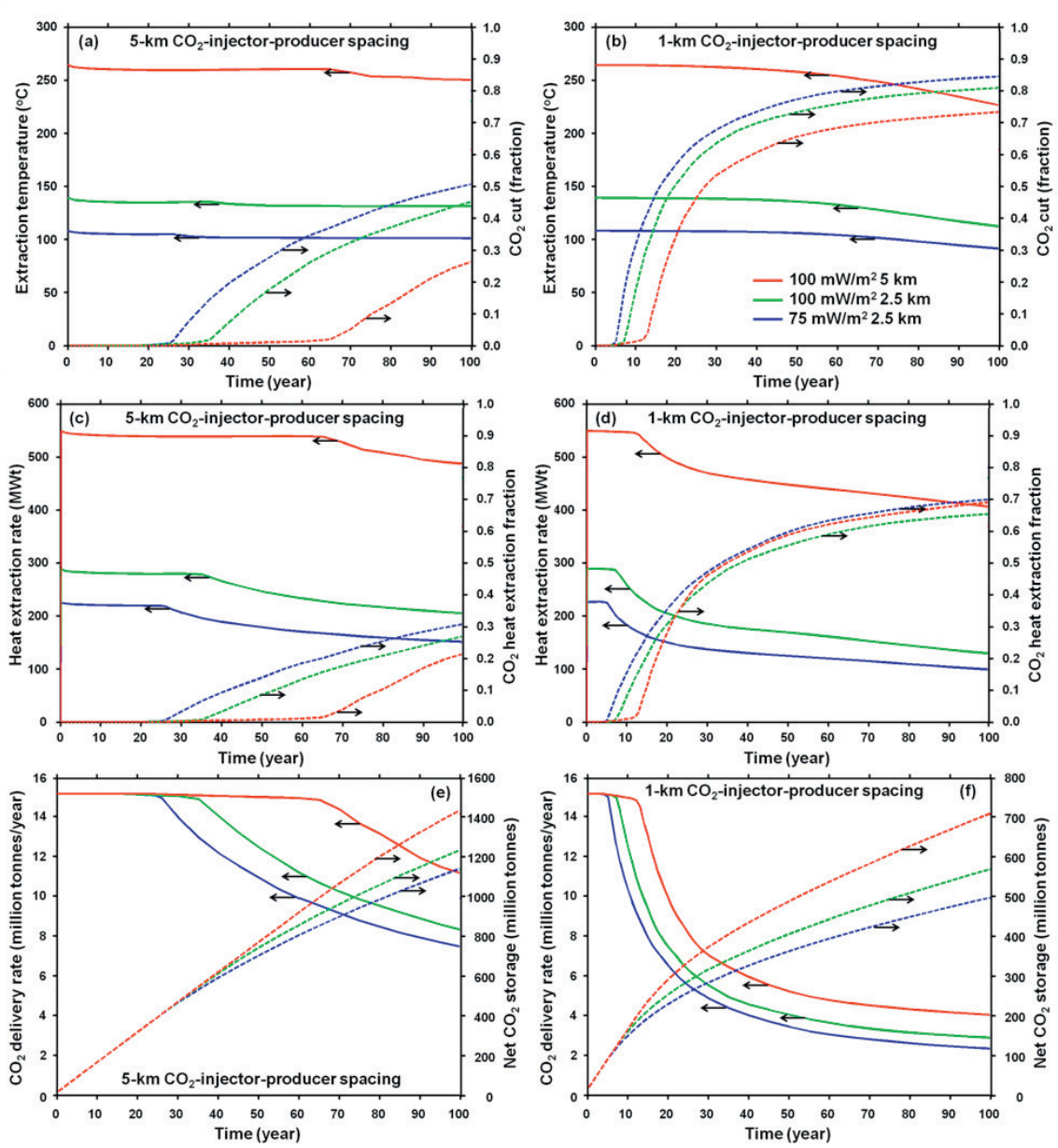

Fig. 3. Histories of extraction temperature and CO_2 cut (a,b); heat extraction rate and CO_2 heat extraction fraction (c,d); and CO_2 delivery rate and net CO_2 storage (e,f) are plotted for case B-2 for large (a,c,e) and small (b,d,f) CO_2-injector-producer spacing.

4.1. Manipulation and control of the CO_2 plume and overpressure

Migration of injected CO_2 is dominated by buoyancy (Fig. 1a). Buoyant flow of CO_2 also dominates where maximum overpressure occurs (Fig. 1c). Rather than occurring at the point of injection, the maximum overpressure occurs above the CO_2 injectors, at the contact between the storage aquifer and the lower caprock. The addition of two

producers pulls the CO_2 plumes towards the center of injection, where they coalesce (Fig. 1b), while the brine injectors create hydraulic barriers (Fig. 1d) that push the CO_2 plumes towards the center of injection. Pull-push manipulation causes the CO_2 plumes to occupy more of the vertical extent of the storage aquifer, and constrains outward migration, with greater utilization of the aquifer pore space. Overpressure in the middle aquifer is identical for these two cases (Fig. 1c and d). The histories of overpressure at the top of the storage aquifer (Fig. 4c), overpressure difference across the caprock (Fig. 5c), and far-field overpressure (Fig. 6c) are the same for these two cases (I-V and B-1). The primary purpose of producing brine and injecting it back into the storage aquifer is to control CO_2 plume migration; however, overpressure is unchanged. A comparison of case I-H with the vertical-well case (I-V) shows the benefit of using horizontal wells to reduce overpressure (Figs. 4, 5, and 6).

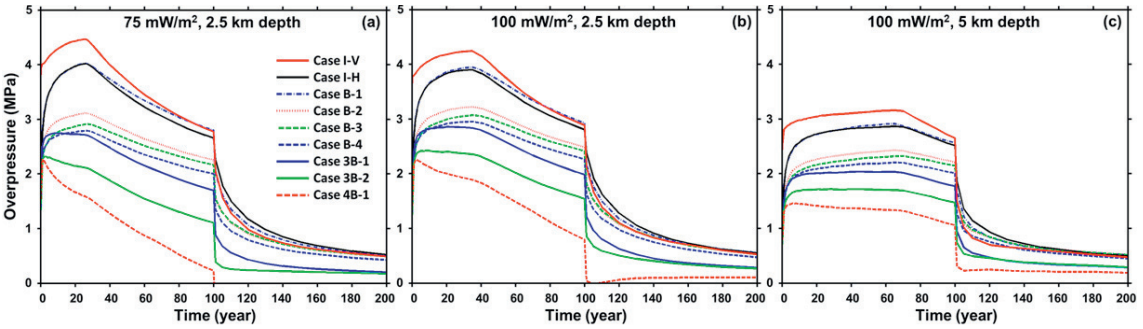

Fig. 4. Histories of maximum overpressure at the top of the storage aquifer above the CO_2 injector are plotted.

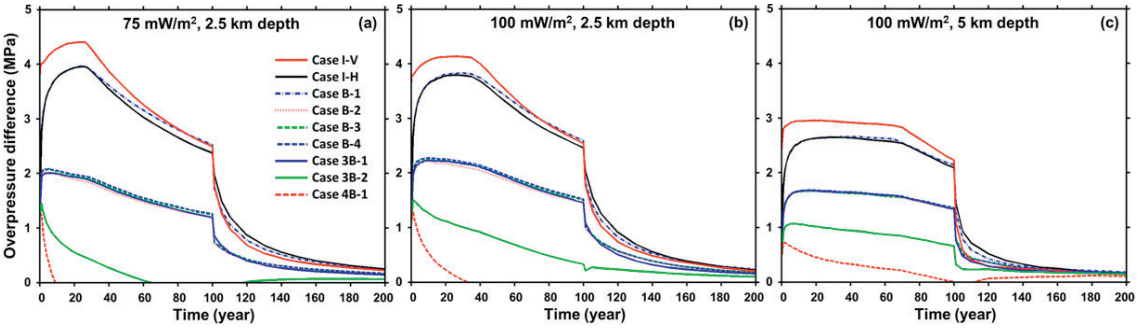

Fig. 5. Histories of overpressure difference across the caprock above the CO_2 injector are plotted.

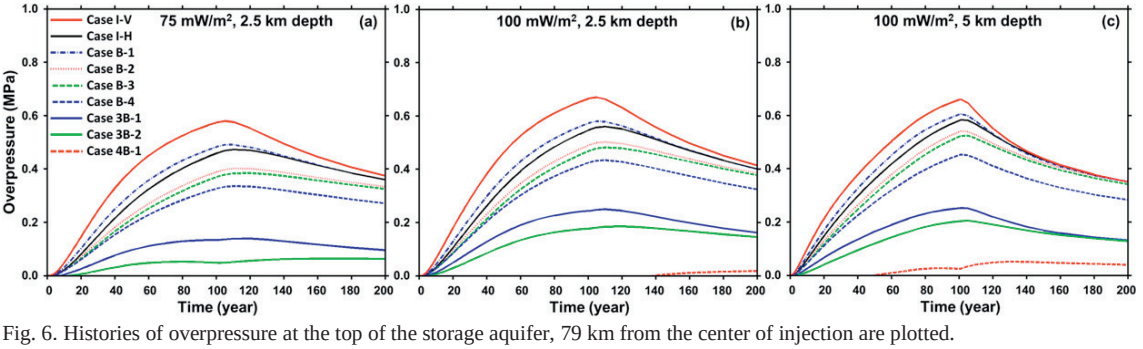

Fig. 6. Histories of overpressure at the top of the storage aquifer, 79 km from the center of injection are plotted.

A comparison of panels a, b, and c in Figs. 4 and 5 illustrates the temperature dependence of overpressure, driven by two different effects. First, hydraulic conductivity increases with temperature, due to the corresponding decrease in viscosity, causing overpressure to decrease with increasing temperature. Second, the viscosity of water decreases more steeply with increasing temperature than does that of supercritical CO_2, causing the mobility ratio

of CO_2 and brine to decrease with temperature. Consequently, preferential CO_2 flow is less pronounced at higher temperatures, which increases CO_2 breakthrough time, causing CO_2 cut to increase more slowly (Fig. 3a). Since the produced CO_2 is recycled, CO_2 delivery rate decreases more quickly for lower temperatures, resulting in less net CO_2 storage (Fig. 3e) and a more rapid decline in overpressure (Figs. 4 and 5). Overpressure peaks when CO_2 first arrives at the producers; thereafter, it declines due to the decreasing CO_2 delivery rate. Because the injection-only cases apply the CO_2 delivery rate history of the corresponding brine production cases, overpressure peaks at the same time as in the brine production cases. Because net CO_2 storage increases with temperature, far-field overpressure increases with temperature (Fig. 6).

Injecting half of the produced brine into the middle aquifer extends the region of overpressure all the way up to the upper caprock, reducing its magnitude in the storage aquifer and lower caprock (Fig. 2); yet, the hydraulic barrier still constrains outward CO_2 migration (Fig. 2). Distributing brine injection over the middle and storage aquifers reduces overpressure at the top of the storage aquifer (Fig. 4). Increasing overpressure in the middle aquifer substantially reduces the overpressure difference across the caprock (Fig. 5c), which reduces the driving force for potential CO_2 leakage through discrete pathways such as abandoned wells or faults. Brine injection in the middle aquifer has a minor effect on far-field overpressure (Fig. 6c) because far-field overpressure is sensitive to net fluid injection. Increasing brine-injector-to-CO_2-injector spacing from 3 to 6 km has a minor impact on decreasing overpressure (cases B-2 and B-3 in Fig. 4). Decreasing the brine injection rate by 34 percent has a minor impact on decreasing overpressure (cases B-3 and B-4 in Fig. 4). Overpressure difference (Fig. 5) is more sensitive to the relative rate of brine injection in the middle and storage aquifers than to the magnitude of those rates.

The most influential brine injection/production strategy is to combine the consumptive use of brine with production/injection ratios > 1, as done in cases 3B-1, 3B-2, and 4B-1, which requires the addition of brine producers, located at the perimeter and spaced 5 km from the brine injectors (Fig. 2b and d). The additional brine producers have little influence on the shape of the CO_2 plume (Figs. 2a and b). The brine injectors create a hydraulic *ridge*, which is a barrier to CO_2 migration and leakage, while the brine producers create a hydraulic *trough*. With high enough production rates, this trough can nullify the hydraulic ridge, causing far-field overpressures to be close to zero (Figs. 2d and 6). This strategy can hydraulically isolate a geothermal-GCS operation from neighboring subsurface activities, which equates to reducing the AoR and pore-space competition. This strategy can also greatly reduce the overpressure difference across the caprock (Fig. 5).

4.2. Production of geothermal energy and water

For all cases, an initial decline in temperature of 3 to 4 ^{o}C is the result of cooler water being drawn down to the producer at the base of the storage aquifer (Fig. 3a and b). After this initial period of thermal mixing, thermal drawdown does not commence until the arrival of CO_2 (Fig. 3a and b). We considered cases representative of the two end-member strategies for integrated geothermal-GCS, starting with the strategy that utilizes CO_2 injection for pressure support of geothermal wells. For large (5-km) CO_2-injector-producer spacing, thermal drawdown is small (4, 4, and 10 ^{o}C) during the 100-year operation period. Heat extraction rate is highest (221, 282, and 541 MWt) when only brine is produced (Fig. 3c), then declines with increasing CO_2 cut because CO_2 carries less heat per unit mass than brine. Small (1-km) CO_2-injector-producer spacing causes early CO_2 breakthrough (Fig. 3b) and recirculation, with a more rapid decline in CO_2 delivery rate (Fig. 3f). Because CO_2 breakthrough occurs earlier, thermal drawdown is faster (Fig. 3b). Heat extraction rate also declines more steeply. Had we taken advantage of the lower viscosity and thermosyphon effect of CO_2, we could have increased the CO_2 production rate to maintain a higher heat extraction rate than shown in Fig. 3d. For cases 3B-1, 3B-2, and 4B-1, thermal breakthrough does not occur at the brine producers during the 100-year operation period, resulting in negligible thermal drawdown. For case 4B-1, total brine production is 1920 kg/sec, resulting in a heat extraction rate of 842, 1072, and 2115 MWt for the low, medium, and high temperature cases. Using GETEM [14] to calculate binary-cycle electrical power production, case 4B-1 is found to generate 35, 62, and 253 MWe for these cases. For the high-temperature case, this power output is 13.3 percent of the 1.9 GWe output from the coal plants that generated the injected CO_2. Annual water production for these cases is listed in Table 1.

5. Conclusions

We have shown how the viability of large-scale GCS may be enhanced through its synergistic integration with geothermal energy and water production. The most challenging implementation barriers facing GCS are energy and water demands for CO_2 capture and overpressure caused by CO_2 injection. We conduct reservoir analyses of horizontal wells in a stack of permeable saline aquifers, separated by impermeable seal units. We analyze the two end-member approaches to utilizing CO_2 in geothermal energy production: one focused on utilizing CO_2 as an efficient working fluid, and the other focused on utilizing CO_2 injection for pressure support of geothermal wells. For the second approach, we consider different pressure-management strategies and develop a generic well pattern with four concentric zones of wells in the storage aquifer: (1) inner brine/CO_2 producers, (2) CO_2 injectors, (3) brine injectors, and (4) outer brine producers; and two zones (3 and 4) in the overlying saline aquifer. This well pattern manipulates the CO_2 plume by pulling and pushing, creates a hydraulic ridge and cap to suppress CO_2 migration and leakage, and creates an outer hydraulic trough to nullify the hydraulic ridge, thereby hydraulically isolating the geothermal-GCS operation from its neighbours, which reduces pore-space competition and the Area of Review (AoR). In addition to managing overpressure, we show how this concept has the potential of producing enough geothermal energy and water to significantly defray the parasitic costs of CO_2 capture.

Acknowledgements

This work was sponsored by the USDOE Fossil Energy, National Energy Technology Laboratory, managed by Andrea McNemar, by the USDOE Geothermal Technologies Program, managed by Hidda Thorsteinsson, by the Carbon Mitigation Initiative at Princeton University, and by the Environmental Protection Agency under Cooperative Agreement RD-83438501. We want to acknowledge Jeff Bielicki and Hyungjin Choi at the University of Minnesota for their GETEM analysis of geothermal electrical power generation. This work was performed under the auspices of the USDOE by LLNL under contract DE-AC52-07NA27344.

References

1. IPPC (Intergovermental Panel on Climate Change), (2005) Special report on carbon dioxide capture and storage. Cambridge University Press, Cambridge UK and New York, NT, USA.
2. Socolow, R.C. and Pacala, S.W. (2006) A Plan to keep carbon in check. *Scientific American*, **295**, 3: 50–57.
3. Buscheck, T.A. (2010) Active management of integrated geothermal-CO_2-storage reservoirs in sedimentary formations: An approach to improve energy recovery and mitigate risk, Proposal in response to DE_FOA-0000336: Energy Production with Innovative Methods of Geothermal Heat Recovery, LLNL-PROP-463758.
4. Buscheck, T.A., Elliot, T.R., Celia, M.A., Chen, M., Hao, Y., Lu, C., Sun, Y. (2012) Integrated, geothermal-CO_2 storage reservoirs: adaptable, multi-stage, sustainable, energy-recovery strategies that reduce carbon intensity and environmental risk, *Proceedings for the Geothermal Resources Council 36th Annual Meeting*, Reno, NV, USA.
5. Bourcier, W.L., Wolery, T.J., Wolfe, T., Haussmann, C., Buscheck, T.A., and Aines, R..D. (2011) A preliminary cost and engineering estimate for desalinating produced formation water associated with carbon dioxide capture and storage, *Int. Journal of Greenhouse Gas Control*, **5**, 1319–1328.
6. Buscheck, T.A., Sun, Y., Chen, M., Hao, Y., Wolery, T.J., Bourcier, W.L., Court, B., Celia, M.A., Friedmann, S.J., and Aines, R.D. (2012) Active CO_2 reservoir management for carbon storage: Analysis of operational strategies to relive pressure buildup and improve injectivity, *Int. Journal of Greenhouse Gas Control*, **6**, 230–245.
7. Buscheck, T.A., Sun, Y., Hao, Y., Wolery, T.J., Bourcier, W.L., Tompson, A.F.B., Jones, E.D., Friedmann, S.J., and Aines, R.D. (2011) Combining brine extraction, desalination, and residual-brine reinjection with CO_2 storage in saline formations: Implications for pressure management, capacity, and risk mitigation, *Energy Procedia* **4**, 4283–4290.
8. Pruess, K. (2006) Enhanced geothermal systems (EGS) using CO_2 as working fluid – a novel approach for generating renewable energy with simultaneous sequestration of carbon. *Geothermics*, **35**, 351–367.
9. Randolph, J.B. and Saar, M.O. (2011) Coupling carbon dioxide sequestration with geothermal energy capture in naturally permeable, porous geologic formations: Implications for CO_2 sequestration. *Energy Procedia*, **4**, 2206–2213.
10. Saar, M.O., Randolph, J.B., and Kuehn, T.H. (2010) Carbon Dioxide-based geothermal energy generation systems and methods related thereto, U.S. Patent Application 20120001429.
11. Court, B., Bandilla, K., Celia, M.A., Buscheck, T.A., Nordbotten, J.M., Dobossy, M., and Jansen, A. (2012) Initial evaluation of advantageous synergies associated with simultaneous brine production and CO_2 geological sequestration, *Int. Journal of Greenhouse Gas Control*, **8**, 9-100.
12. Zoback, M.D. and Gorelick, S.M. (2012) Earthquake triggering and large-scale geologic storage of carbon dioxide, Proceedings of the National Academy of Sciences, **109**, 26, 10164–10168.
13. Nitao (1998) Reference manual for the NUFT flow and transport code, v3.0, Lawrence Livermore Nat. Lab., UCRL-MA-130651-REV-1.
14. DOE (2012) GETEM – Geothermal electricity technology evaluation model, August 2012 Beta, USDOE Geothermal Technologies Program.